

# Energy Level Statistics and Lyapunov Exponent in the Stadium Billiard

by

David Samuel Gloss II

Submitted to the Department of Physics  
in partial fulfillment of the requirements for the degree of

Master of Science in Physics

at the

MASSACHUSETTS INSTITUTE OF TECHNOLOGY

June 1995

© Massachusetts Institute of Technology 1995. All rights reserved.

Author \_\_\_\_\_  
Department of Physics  
June 2, 1995

Certified by \_\_\_\_\_  
Michel Baranger  
Professor  
Thesis Supervisor

Accepted by \_\_\_\_\_  
George Koster  
Chairman, Departmental Committee on Graduate Students

MASSACHUSETTS INSTITUTE  
OF TECHNOLOGY

JUN 26 1995

LIBRARIES

ARCHIVES

# Energy Level Statistics and Lyapunov Exponent in the Stadium Billiard

by

David Samuel Gloss II

Submitted to the Department of Physics  
on June 2, 1995, in partial fulfillment of the  
requirements for the degree of  
Master of Science in Physics

## Abstract

I have found a new method for investigating energy level statistics that allows statistically significant results to be obtained for much smaller numbers of energy levels than is normally needed. This was made possible by my discovery that the Brody distribution is the Weibul distribution for which the Anderson-Darling statistic is applicable. This new method allowed me to investigate the energy level statistics in the stadium billiard in the region between G.O.E. and Poisson statistics where I found statistically significant deviations from the Brody distribution for very small quantum number  $n$ . Lastly, I have tentatively found a simple relation between the Lyapunov exponent and the Brody distribution parameter.

Thesis Supervisor: Michel Baranger

Title: Professor

## Acknowledgments

I would like to thank Yumi Sera for her love, Raissa D'Souza for being the “typical grad. student” Eric Heller for his computer program, Miriam Wardle for her help with statistics, and Michel Baranger for his patience.

I would also like to thank the Roman who reminded me that MITans are like any other people: *Δυὸ ταῦτα ἐξελεῖν τῶν ἀνθρώπων, φησὶν καὶ ἀπιστιᾶν*

This research was supported by a John Lyons fellowship.

# Chapter 1

## Background

### 1.1 Introduction and Goals

Quantum chaos is the study of chaos in quantum mechanics that is like that of classical systems[16]. The Riemann zeta function is the best example I know: it is seemingly unpredictable and analytically smooth. The stadium billiard is two half circles of radius  $r$  joined by two parallel straight lines of length  $2a$ ; it is another quantum chaotic system, please see fig. 1-1. In it, the chaos is seen in the energy levels. For example, the nodal patterns of many of the wave functions are chaotic[20]. The stadium billiard is also interesting because the analogous classical system is chaotic for all non-zero aspect ratio( $\gamma = \frac{a}{r}$ ). In the classical case, the billiard is chaotic, because the trajectory of a ball bouncing inside the stadium is unpredictable.

The most simple question of the relationship between the regular  $\gamma = 0$  and the

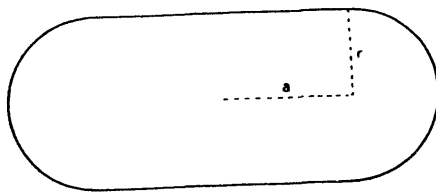


Figure 1-1: The stadium billiard

chaotic  $\gamma \neq 0$  is how small does  $\gamma$  need to be to feel the presence of the regular region? This is the main goal of my thesis.

The succeeding sections of this chapter will be devoted to a few concepts. It will, I believe, enable the reader unfamiliar with the complexities of what I am undertaking to be conversant with some things the typical graduate student in physics may not have encountered; and thus, be able to judge the second chapter, my contribution.

## 1.2 Energy Levels

My thesis is primarily about the statistics of energy levels, so, I thought, it might be fitting to introduce this subject first. My treatment in this section is mainly based on an excellent introduction to the topic of quantum chaos[16]. First, we have some list of energies for a system, written in the form of a staircase  $N(E) = \sum_n \Theta(E - E_n)$  where  $\Theta$  is the step function and the spectral density  $d(E) = \sum_n \delta(E - E_n)$ . For an ergodic system, the cumulative energy levels of a system is approximately equal to the area times the total phase space below that energy divided by the phase space unit cell  $h^d$ . An ergodic system is one whose trajectories in phase space are dense. For the stadium billiard, the phase space is  $\pi p^2 = 2\pi m E_{max}$ , but, as we are solving the Schrodinger equation,  $2\pi m E_{max} = \pi \hbar^2 k_{max}^2$ . Taking what we have just learned about ergodic systems, of which the stadium certainly is one,  $N = \frac{A k_{max}^2}{4\pi}$ , setting the area to be a constant. The constant  $4 + \pi$  has been chosen to compare with a previous work[17].

Weyl's formula gives the next better approximation to the next order in  $k$ :  $N(k) = \frac{A k^2}{4\pi} + \frac{P}{2\pi}$  where  $P$  is the perimeter of the boundary. Further information is entirely dependent on the topology of the situation and is not at all trivial to calculate. Papers published in the last two years have solved this problem theoretically, but have only been tested against one of the two possible cases[1][27].

From a knowledge of the step function, one then calculates the distance to the nearest neighbor. If one looks at the ensemble of nearest neighbor distances, one can calculate a probability distribution  $P(x)dx$  of finding two levels a distance  $dx$

apart. A simple example of this would occur for the harmonic oscillator, where the probability distribution would just be a delta function. Another related measure is called the spectral distribution  $Q(x)dx$  which is the probability of finding an energy level within a distance  $dx$  of any given level. The completely random energy level distribution with average density 1 would have  $Q(x)$  equal to one as the probability of finding an energy level at any distance is completely independent of any other energy level.  $P$  and  $Q$  are related by  $P(x) = Q(x) \exp[-\int dx' Q(x')]$ .

For a random system of average density one, a Poisson spacing is found. An integrable system is one for which there are other constants of motion besides the energy. A completely integrable system would be a system that one could find a canonical transformation of the Hamiltonian to reduce half the coordinates to constants except time like Hamilton-Jacobi theory from classical mechanics. Integrable systems are found to have Poisson spacing of the energy levels which is quite surprising.

For many time-reversal invariant systems, the Gaussian Orthogonal Ensemble applies. The G.O.E. is just the canonical ensemble for the velocity distribution for particles in a gas

$$\exp[-A \sum_{jk} (h_{jk})^2 - B \sum_j H_{jj} - c] \prod_{l \leq n} dH_{ln}$$

with one important difference,  $B = 0$ . The main result of the theory is contained in finding  $P$  that applies to many nuclear systems. There is no known closed form that has a simple expression, but many use Wigner's surmise  $P(x) \simeq \frac{\pi}{2} x e^{-\frac{\pi x^2}{4}}$ . It is within a few percent of the exact result; this is sufficient for most purposes as most data are in the form of crude histograms.

An important question is how these systems fluctuate from the average spacing of energy levels. This question be approached by considering "unfolding" of the energy spectrum[7]. Before one considers fluctuations, it would be nice to only look at the fluctuating part in a universal way. For  $N(E)$  being the number of energy levels found equal to or below the energy  $E$ ,  $N(E) = N_{average}(E) + N_{fluctuating}(E)$ , one wants to compare the fluctuation patterns of different parts of the system whose corresponding average behaviors are not the same. One maps the energies  $E_i \mapsto x_i$  by  $x_i = N_{average}(E_i)$ . What this accomplishes is that the sequence  $x_i$  has on the average

a constant mean spacing of one which can be easily seen

$$N_{av}(E) = \int_0^E \rho'_{av} E' dE' = \int_0^x dx' = x = N_{av}(\hat{x})$$

where  $\rho$  is the density of energy levels. An example of the unfolding of an energy staircase would be the unfluctuating case of  $E_k = k^2(k \in \mathcal{N})$ . Here, one transforms  $N_{av}(E) = \sqrt{(E)} = k = x_k$  to get a sequence of equally spaced points, a “picket fence”.

The Brody distribution interpolates between Poisson statistics and the Wigner surmise[11]. This statistic for the nearest neighbor spacing is

$$P_\omega(\Delta E) = A(\Delta E)^\omega \exp(-\alpha(\Delta E)^{1+\omega})$$

where  $A = (1 + \omega)\alpha$  and  $\alpha = [\Gamma(\frac{2+\omega}{1+\omega})]^{1+\omega}$ .  $\omega$  is found by fitting the data by least squares. For Poisson, G.O.E. and Wigner’s surmise, the values for  $\omega$  are 0, 0.953, and 1, respectively. For generic data, A is just a parameter that fit the data. In particular, for fitting a generic histogram, one must multiply the probability distribution by some constant to fit the data: this implies that we can effectively throw out this constant. This is the two-parameter Weibul distribution

$$\frac{k}{\beta} \left(\frac{x}{\beta}\right)^k e^{-\left(\frac{x}{\beta}\right)^k}$$

The Weibul distribution is normally encountered in failure analysis. In a later section, I hope to show why writing the distribution in a form familiar to a mathematician is useful.

## 1.3 Ergodicity

This section tries to show the place of K-flows in the spectrum of statistical mechanics. In appendix A, there will be enough mathematical details for the interested reader to be able to understand the concept of a K-flow in a rigorous mathematical sense. I have not included it here, so as not to impair the clarity of the essential concepts. The papers in the literature about K-flows are either cryptic or are in Russian, so I thought the appendix useful.

In the microcanonical distribution from elementary statistical mechanics, the entire system can be represented as a point in phase space that is a function of time.

The motion of the system in phase space remains on a surface of constant energy. If there are other constants of motion beside the energy, the motion of the system in phase space will be confined to some part of the energy surface. If there are no other constants, the system will pass arbitrarily close to an arbitrary point on the surface if given a long enough time.

Two uncoupled harmonic oscillators provide an example of both these situations[4]. The Hamiltonian for the system is  $H = \frac{1}{2}(p_1^2 + \omega_1^2 q_1^2) + \frac{1}{2}(p_2^2 + \omega_2^2 q_2^2)$  As they are uncoupled, they can each be considered separately, as eliminating the time will clearly show. If the ratio of the frequencies is rational, the path of the system in phase space will be some closed curve with a finite number of self-intersections. The energy surface is thus partitioned into areas visited by the closed curve and those not so visited. Now, if the ratio is not rational, the curve of their trajectories will not be periodic, it will completely fill the torus representing the phase space of the two-oscillator system. This is what it means to be ergodic. In more mathematical terms, if you prefer, one could say if we represent the system by  $\mathcal{S}(t)$  in phase space,  $\lim_{t \rightarrow \infty} \int \frac{1}{t} dt' g(\mathcal{S}(t')) = \frac{\int d\mathcal{S}[H(\mathcal{S})-E]g(\mathcal{S})}{\int d\mathcal{S}[H(\mathcal{S})-E]}$ [24].

The ergodic theorem is actually due to Birkhoff. It says that given a dynamical function  $d(x)$  integrable over the phase space, if the space cannot be decomposed into two invariant regions different from measure zero or one, then

- i)  $\bar{d}(x)$  is constant almost everywhere
- ii)  $\bar{d}(x) = \langle d \rangle$

Metric indecomposability expresses the fact that no trajectory can be confined to some portion of phase space. I should note that the phase space is here defined as anything that we can define an invariant measure on. The latter of the two properties expresses the fact that almost every trajectory spends an equal proportion of its time in equal regions everywhere in phase space. The importance of the theorem is also due to the latter property, because, often, it is much easier to calculate the space average than the time average.

A mixing system is experienced in our everyday lives. It means what we might think it would: it describes a system that gets mixed up. Take for example, making



chocolate milk. We take a two substances milk and chocolate and after mixing the two we find them in the proportions equal to the proportions of them unmixed everywhere we care to look. In terms of phase space, the system can be said to spread throughout the entire phase space. Two points in proximity to one another in phase space may move apart, or they might not. In relation to an ergodic system, we are no longer confined to a surface that we will cover in phase space, but to the entire space. A small error in measurement can propagate in time and introduce large enough errors so that long time predictions are impossible. Given two compact regions of the phase space  $A(t)$ ,  $B(t)$ , and the measure  $\mu$ ,  $\lim_{t \rightarrow \infty} \frac{\mu(A(t) \cap B(0))}{\mu(B(0))} = \mu(A(0))$ . It is clear that something that is mixing must be ergodic. Just consider the case of an invariant  $A$  and let  $B=A$ , plugging into the equation, we get that  $\mu(A) = \mu(A)^2$  so that  $\mu(A)$  must be equal zero or one. Hence the system is ergodic. Ergodicity does not, on the other hand, imply mixing.

A K-system is a mixing system with the property that most orbits from points close together separate, on average, exponentially with time. The system is governed by casual equations of motion, but the time evolution of a generic point in phase space is so irregular, it may seem random [10]. The entropy defined relative to a finite partition is the entropy summed over each of the partitions. Normally, one thinks of  $S = - \sum_i P(A_i) \log P(A_i)$ ; here we are saying that one chooses what the sets  $A$  are, so instead of  $S$  we have  $S(A)$ . A K-system is one for which the entropy relative to any finite partition is positive.

The Kolmogorov-Sinai entropy is the maximum of  $S(A)$  taken over all finite partitions. K-systems, thus, have a positive K-S entropy. The K-S entropy is an intrinsic quantity associated with the dynamical system considered as a whole at a given energy. It is related to the mean rate of exponential separation of orbits.

A system with the B-property has the property that any finite partition gives the K-S entropy. Clearly, if the K-S is the maximum over all partitions, then all partitions in this case have the same entropy.

I would like to note that the statistical mechanics we studied is based on the following idea by Boltzmann: the infinite time average of a microscopic quantity

is the corresponding macroscopic property. This can only be true for systems in equilibrium, where the macroscopic quantities are stationary. This is rather weak, because the time evolution is of primal importance in any area of macroscopic physics. The mixing system provides something that is a little better in this regard.

If one considers the ensemble average as the *a priori* concept that defines a macroscopic function, then statistical mechanics is predicated on firmer ground. At some time an ensemble is constructed. If the system is of the mixing type, the ensemble will eventually spread to cover the energy surface uniformly and come to thermal equilibrium.

## 1.4 Singular Value Decomposition

Another topic that may be unknown to the average graduate student physicist is a mathematical method for solving equations. This method is useful when one has matrices  $\vec{A} \star \vec{x} = \vec{b}$  when  $\vec{b}$  is very singular. My treatment here is based on two excellent books on the subject, and, though brief, provides, I hope, a good enough summary for one to accept its legitimacy[18][25].

Given a matrix  $A_{m,n}$  with  $q = \min m, n$ , there exists three matrices:  $U_{m,m}$  and  $V_{n,n}$  both unitary and  $W_{m,n}$  diagonal with elements  $w_{i,i} \geq w_{i+1,i+1}$  for all  $i \leq q$ . These diagonal elements are called the singular values; they are interesting because they are the non-negative square roots of the  $q$  largest eigenvalues of either  $AA^*$  or  $A^*A$ . The remaining eigenvalues of  $AA^*$  and  $A^*A$ , if any, are zero.

As a computational device, the way singular value decomposition works uses the fact that  $A$  can be broken up into three matrices. For the  $w_j$ , it is likely that some are very small but non-zero. In such a case, direct solution may lead to a poor approximation to  $b$  due to the large components of  $A$ . In such cases, it is very often better to just set the small  $w_j$  to zero. This means that one can throw away a combination of equations that are so small that they are corrupted by roundoff error. It normally pulls the solution vector away towards infinity, compounding the roundoff error and making the overall solution poorer.

There is some subspace of  $b$  that  $x$  can be mapped by  $A$  onto. Now if  $b$  is in the range of  $A$ , then replace  $w_j^{-1}$  by 0 if  $w_j$  is 0 and

$$x = VW^{-1}U^Tb$$

If  $b$  is not in the range of  $A$ , one can find the closest possible  $x$  in the least squares sense. Similarly to the direct solution, zeroing of the small  $w_j$  usually leads to a better approximation of  $b$ .

## 1.5 Empirical Distribution Function

In order to test whether the statistics that I think should be the correct one, most physicists would do a chi-squared fit of the nearest neighbor energy differences histogram to the probability distribution. In this case, I don't believe that it is such a good idea. My data has between 20 and 200 points in it; the partition for a 0.05 confidence level would have at most 12 cells based on the estimate with  $M$  cells and  $n$  observations  $M = 2n^{\frac{2}{5}}$ [23]. This leads to some averaging of data and consequent loss of information. The tests I want to use do no such averaging, and, as such, no information is lost by making bins.

To test the Weibul distribution with empirical distribution function statistics(E.D.F.), one first transforms it into the extreme-value distribution[28], by the transformation  $Y_i = -\log X_i$  for observations  $X_i$ . The cdf becomes  $F(y) = \exp(-\exp(-\frac{y-\phi}{\theta}))$  where  $\theta = 1/m$  and  $\phi = -\log\beta$ . Now, arrange the  $Y_i$  in ascending order.

There are two parameters to be estimated. This is done by iteratively solving for  $\theta$  by

$$\theta = \sum_j \frac{Y_j}{n} - \sum_j Y_j \exp(-\frac{Y_j}{\theta}) / \sum_j \exp(-\frac{Y_j}{\theta})$$

and then solving for  $\phi$  using

$$\phi = -\theta \log[\sum_j \exp(-\frac{Y_j}{\theta})].$$

I then make a transformation of  $Z_i = F(X_i)$  for the cdf  $F$ . The set  $Z$  should now be uniformly distributed. In the case of the extremal distribution it takes on the form  $F(X) = \exp[-\exp\frac{x-\phi}{\theta}]$ . For exponential distributions, the best statistic for a wide variety of situations is the Anderson-Darling statistic  $A^2$  which I can use to obtain a

confidence level.

Now, as this is a relatively sophisticated statistic, I am free to take full advantage of its power and deal with small groups of energy levels and still statistically significant data. I have used this to my advantage, using only about twenty points for a variety of cases.

## 1.6 Review of Stadium Literature

The history of the stadium billiard is over twenty years long. Research was initially generated with the proof by Bunimovich that the stadium was a B-system[13]. His proof was accomplished by considering boundary shapes for a general class of billiards which do not contain any dispersing components. In this case, dispersing means that trajectories diverge. It was also assumed that the billiard had at least one focus, as it had previously been proved that polygonal shapes which do not have any focusing components have zero entropy. It was further assumed that the focusing part of the boundary would have a constant curvature.

The border, therefore, could be made up of straight segments and segments from a circle with the interior of the circle pointing toward the interior of the billiard. The proof itself basically considers successive reflections of bundles of trajectories to prove the B-property. A bundle contracts after reflection from a circular section and then expands in such a way that timing of later focusing is impossible to know, thus proving the system to be stochastic. The fact that these objects have the B-property relatively easily led to the proof of the K-property [12]

These papers by Bunimovich are so famous that often a simple example of the kind of objects included in his paper, the stadium, is called the Bunimovich stadium, because of all the interest these papers generated. The papers are of such importance because the K-property implies that the object has positive entropy. The B-property implies that this entropy is constant almost everywhere. The people who investigated the Lyapunov exponent(a measure of entropy) incorrectly thought ergodicity implied the Lyapunov exponent was constant[5].

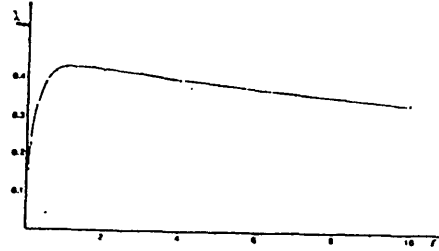


Figure 1-2: Maximal Lyapunov exponent vs. aspect ratio

The first numerical investigation of the billiard computed the maximal Lyapunov exponent as a function of the aspect ratio ( $\gamma = \frac{a}{r}$ ) of the stadium[5]. Please consider fig. 1-2. The maximal Lyapunov exponent was calculated by

$$\lim_{t \rightarrow \infty} \ln \|dT_x^t(e)\| \text{ where } T = x^t$$

is the flow along the tangent space. It measures the mean rate of exponential divergence for the bundle of trajectories passing through the point  $x$ . If it is positive, the system can be considered chaotic, because even extremely close initial conditions will show an exponential divergence of trajectories. This means that trajectories beginning closer than can be resolved will eventually lead to different trajectories; it will be impossible to predict the full trajectory from its initial conditions. The fact that the maximal Lyapunov exponent is constant for a given aspect ratio serves as a key point of comparison.

There was a conjecture that Gaussian orthogonal ensemble statistics should be seen in a classically chaotic system[16]. The stadium, which is stochastic for all non-zero aspect ratio, seemed to be a natural choice to test this hypothesis. In a landmark paper that strengthened the near universality of G.O.E. statistics, the cases of aspect ratio 0 and 1 were investigated[20] and G.O.E. statistic were precisely found for aspect ratio 1. Please acquaint yourself with figs. 1-3 and 1-4.

These figures show  $N(\Delta E) vs. \Delta E$  where  $N$  is the probability to be within a certain energy distance of a specified level. In the circular case (aspect ratio 0), the spacings behave like a Poisson distribution. This is to be expected, because the energy levels should just be the zeroes of the Bessel functions.

The explicit connection between the billiard and G.O.E. statistics was not made

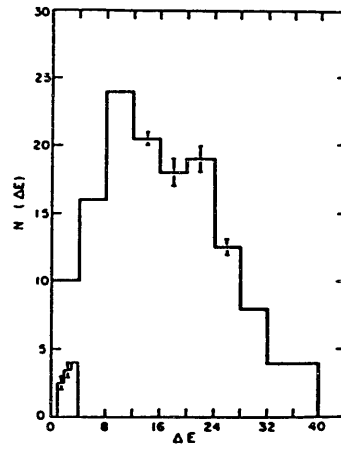


Figure 1-3:  $N$  for aspect ratio 0

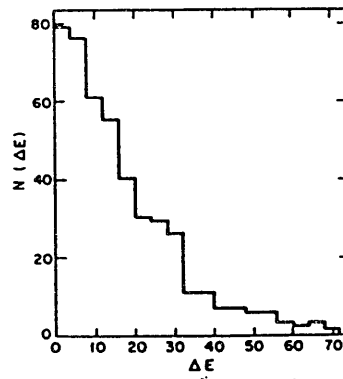


Figure 1-4:  $N$  for aspect ratio 1

until a little later[9]. The data and the G.O.E. curve were compared using the Dyson-Mehta statistic( $\Delta_3$ ), the probability distribution, the variance, the skewness, and the kurtosis. The Dyson-Mehta statistic measures the long range correlations in energy levels and is defined as the local average of the mean square deviation of the spectral staircase  $\sum \Theta(E - E_n)$  from the straight line fitted to an energy range corresponding to  $L$  mean level spacings. All the tests fit G.O.E.

The original paper that showed G.O.E. statistics in the stadium only considered the odd-odd symmetry states. There should be four symmetry classes as the stadium is invariant about two axes. All four classes were shown to follow G.O.E. statistics[9]. The symmetry that most closely followed the overall statistics was the odd-odd symmetry class. Later papers almost invariably only consider the odd-odd states, for they seem to be representative of the whole spectrum. The number of energy levels considered in the paper that considered all four symmetry classes was 800 per symmetry class, so that the statistics generated would be considered valid. The G.O.E. prediction was found in all statistics measured. In the same year, another article found the same situation with a different K-system billiard[8], thus, reaffirming the universality of G.O.E. statistics. Later examples were found that ended these thoughts of universality. One such example is a billiard on a surface of constant negative curvature [3] where there can be near degeneracies in small samples. If G.O.E. were applicable, this would be highly unusual.

A kind of regular wave function of the billiard is often called a “whispering gallery” orbit, because it remains localized near the edge. These were explained by considering it a “scar” of an unstable periodic orbit[30]. There was an explanation of both the quantum and classical systems and a comparison of the results[14]. They showed that there was a very strong agreement between the predictions of classical and quantum mechanics for states in the stadium other than the vertically directed unstable periodic orbits. There were also similarities between the asymptotic limit of the expectation values and the rate at which those values were reached. This implies that the quantum- classical correspondence will only break down in infinite time.

In what was later an important Ph.D thesis in this field, the cases of aspect

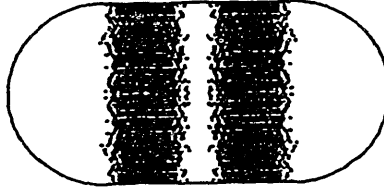


Figure 1-5: An example of a regular orbit

ratio 0 and 1 were closely investigated[21]. It established the use of a particular computational method that left some 1 percent of the eigenvalues erroneous and 1percent of the eigenvalues missed. A new more foolproof technique was called for and was found[17]. The author of this technique told me it can be troublesome as it has trouble with dealing with energy levels that are close together. His method was used in my thesis and I did have trouble gathering data, but was able to get results after some tribulation. I had to closely examine the predicted  $N_{weyl}$  to see if I had missed a level to get some idea where the missed level was and reinvestigate the area closely to find it.

Both the level clustering and irregular wave functions with uniform distributions of nodal lines had been predicted[6] for aspect ratio greater than zero. This uniform distribution of lines is an indication of an isotropic distribution of wavevectors. This fact was taken up in the computer program I have used.

The other regular wave functions were localized states correspond to classical motion of almost perpendicular reflections from the straight part of the stadium and to the pseudo-regular states that appear diamond shaped and localized near the boundary[29]. Please consider fig. 1-5[17]. These regular states had a relatively simple explanation. In the time frame of one of the coordinates, the other can be considered constant. This means that the Schrodinger equation can be solved by considering the following Hamiltonian:  $H = -\frac{(\hbar)^2}{2m^2} \frac{d^2}{dy^2} + V(y)$  where  $v(y) = 0$  or  $\infty$  for  $|y| < y_0$  or  $|y| > y_0$  respectively.  $y_0 = R$  for  $|x| < 0$  and  $\sqrt{R^2 - (|x| - a)}$  for  $a \leq |x| \leq a + R$  The system has solutions  $\phi_n = -\frac{1}{\sqrt{y_0}} \sin \frac{n\pi}{2} (\frac{y}{y_0} + 1)$ . These results were verified by others who considered the propagation of an initially localized Gaussian in the stadium[14].



The semi-classical trajectories were allowed to propagate in time and it was found that the quantum mechanical and semi-classical systems agreed[30] with a surprising accuracy. The exact quantum mechanical auto-correlation function was compared to that of the semi-classical approximation and every detail was captured. The semi-classical approximation to the Green's function failed along certain trajectories. In particular, for the case of striking the point of intersection between the straight edge and the circular part of the stadium, a fold would develop in the trajectories. This fold would invalidate the use of the semi-classical Green's function.

Eventually, one would hope that enough interest would be generated for someone to find a physical system that could test all the numerical work that had been done. Such a test was performed nearly twenty years after the first numerical work on the stadium was published[15]. The experimenters found frequencies in a microwave cavity made from superconducting niobium held at very low temperatures. For a flat enough microwave resonator, Maxwell's equations reduce to the Schrodinger equation of a free particle except at the boundary. If the boundary is superconducting, then the waves bounce off the stadium as if they encountered an infinite potential which gives the desired boundary conditions. In this case, the frequency that one could determine if one has another known frequency nearby is at worst  $\Delta f = 10^{-5} f$ . This high quality value means it is very likely no levels were missed.

If one considers the trajectories where the wavefunction bounces between one wall and the next, one can calculate the cumulative level density by considering the semi-classical propagator of the orbits that do not leave the rectangular section of the boundary. If  $N^{bounce}$  is the number of bouncing ball orbits,  $N - N_{weyl}$ , the result is  $N^{bounce} = (\frac{1}{2\pi})^{\frac{3}{2}} \frac{a}{r} \sqrt{2kr} \sum_{m=1}^{\infty} m^{-\frac{3}{2}} \cos[2mkr - \frac{3\pi}{4}]$ . The experimenters found excellent agreement with the experimental calculation of 1060 eigenmodes and that predicted by their semi-classical calculation.

The case that they considered was for aspect ratio 1.8. They followed the Brody distribution in considering  $N(\Delta E) vs. \Delta E$  and found that it did not follow G.O.E. statistics. The fit is not far off, with the Brody parameter being  $0.82 \pm 0.07$ .

The last paper relevant to the stadium that I have chosen to relate to the reader,

is one that has the odd-odd symmetry calculation of the effect of multiple bounces on the semi-classical Green's function[27]. The semi-classical Green's function is only an integral away from the semi-classical level density. They also considered such things as unstable periodic orbits. The contribution of isolated unstable periodic orbits was similar in form to the oscillatory contributions to the bouncing ball orbits. Finally, they considered the family of neutral periodic orbits whose orbits are almost closed, or "whispering gallery" orbits. The contribution to all these things in the Dyson-Mehta statistic was compared to the data for microwave stadium and was in good agreement. The already published cases of aspect ratio 1 and 0 were not compared: the case of 0 is a completely degenerate case, as there should be no bouncing ball orbits which are due to reflections off the straight part of the stadium. A similar paper was done on the full stadium[1].

A recent paper examining the virtual paths inside a mirror cabinet made in the shape of a stadium is amusing. The virtual image boundaries for other mirror cabinets known to possess non-chaotic dynamics are smooth for all orders, while for the stadium, they seem to be fractal in nature[19].

# Chapter 2

## Method and Results

### 2.1 Method

I would like to solve the Schrodinger equation for the stadium billiard:  $(\nabla^2 + k^2)\Psi = 0$  where the solution vanishes on the boundary of the stadium.

The solutions of the equation are obviously of the form of plane waves which trivially solve the equation[17]. I form a basis of odd-odd states so that

$$\Psi = \sum c_n \sin(k_{x,n}x) \sin(k_{y,n}y)$$

where  $k_{x,n} = k \cos \theta_n$ ,  $k_{y,n} = k \sin \theta_n$ , and  $\theta_n$  is the angle between an arbitrarily chosen wavevector  $k$  and the wavevector of the plane wave. This angle is then slowly increased in equal increments until it returns to itself (as  $\frac{\pi}{2} = 0$ ). I choose the odd-odd states so that I can compare with what little has been published before in this area and because this symmetry seems to most closely follow the statistics of the overall case. I temporarily assume that for a chosen value of  $k$ , a solution exists.

Now, if a solution exists, it should be zero on the boundary. For  $N$  plane waves, I can force  $N$  points to be whatever I choose. So, I choose  $N-1$  points to be zero on the boundary and 1 point to be one inside. The point inside normalizes the wave function. The points along the boundary are chosen to be equally spaced along the outer edge. The interior point is randomly chosen to be somewhere within the stadium. I can consider this to be  $N$  equations with  $N$  unknowns: I can think of it as  $\Psi x = b$ , where  $\Psi$  is the values along the points,  $b$  is zero everywhere except one entry of one and  $x$

are the coefficients to be determined. As this is quite singular, I use singular value decomposition to determine  $x$ ; Gauss-Jordan elimination would never find the answer.

Now, I find the tension of the function by equally spacing five times the number of points, evaluating the square of  $\Psi$  at each point, and adding the results. The tension should exhibit deep minima when I am close to a real eigenvalue of the Schrodinger equation.

In this way, I should be able to create a list of the energy levels for specified values of  $\gamma = R/L$ . I can then find the statistics of the energy levels and compare it to the already published values of the Lyapunov exponents for the function.

I have modified a version of the program Heller used[17]. The modified program is contained in appendix B as it is possible that it will prove useful for future work. It is necessary to check the vicinity of local minima and shallow minima for points that one might have missed. This can be accomplished by looking at the difference of  $N - N_{weyl}$ . When it drifts to definitely negative and stays there, the program has missed a level. I would like to note that Heller does not include the possibility of evanescent waves in the stadium. In this context, an evanescent wave is of the form of a hyperbolic sine. This could occur by  $k^2 = k_x^2 + k_y^2$  if one or the other of  $k_x$  or  $k_y$  were imaginary. In a personal communication with me, he assured me that they were not necessary to form a complete basis for the stadium.

## 2.2 Results

The first and most basic result is that of whether there are local minima of the tension. Local minima are necessary to find the energy eigenvalues. In a paper using the same area and aspect ratio, one of the energy levels listed is 119.389[17], please consider fig.2-1 which shows a local minimum for the tension at the stated place.

I thought it might be interesting to look at the tension for a large scale so please consider fig.2-2.

It is relatively clear where the local minima are which contain the energy levels.

Once I have a list of the energy levels, I need to know whether they have different

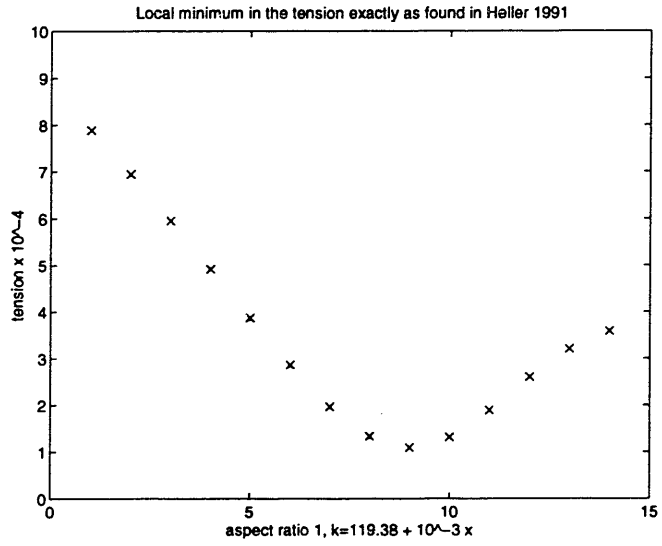


Figure 2-1: Local minimum of the tension

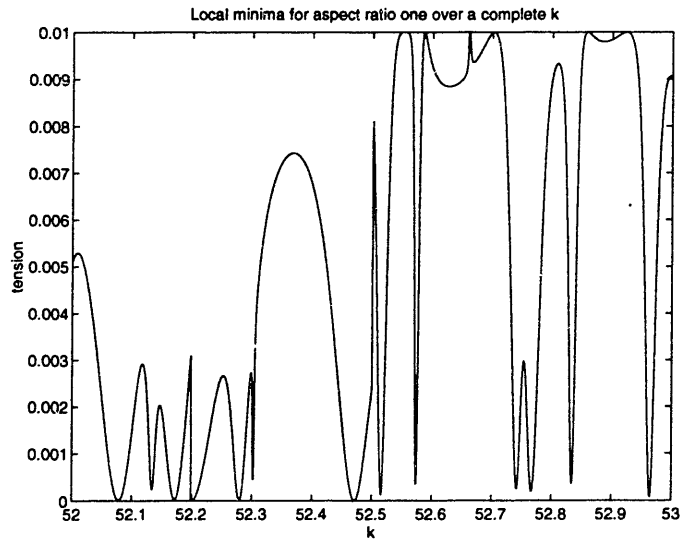


Figure 2-2: Local minima of the tension over a larger scale

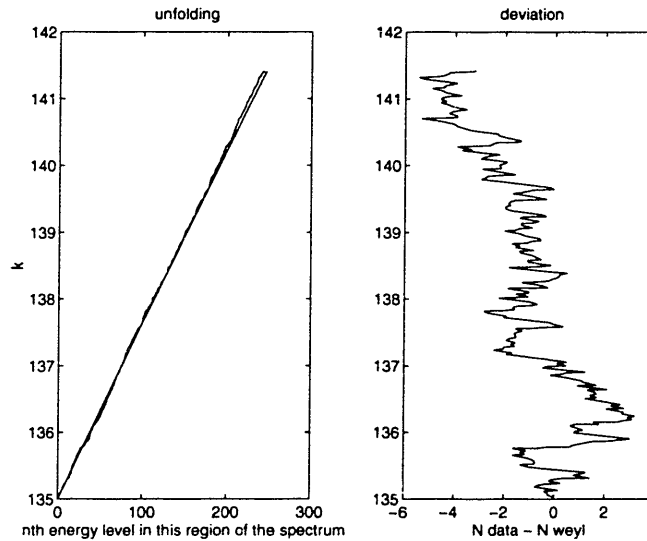


Figure 2-3: Unfolding of my data

average spacing for different parts of the energy spectrum. If they do, they need to be “unfolded”. I have plotted both  $N_{weyl}$  and my data on the left and the difference between my data and  $N_{weyl}$  on the right. Please see fig. 2-3. As we can see the Weyl curve is straight so that the levels do not need to be unfolded. The oscillation of the difference is to be expected; the negative drift can only mean that I have missed some levels. Normally care must be taken so that a level is not missed, but in this case I could not find the missing levels. I think the reason for missing some levels is that the solutions have become so complex that my basis does not cover them. To test this hypothesis, I have attempted to find the energy levels in a much higher energy band and found that I could find only about 10 percent of of the theoretical number of levels. I thought that for high energies the “bouncing ball” orbits which are localized between the straight sections of the stadium would be the only ones I could find. This makes perfect sense, because about 10 percent of the levels have this regularity[16]. So, this case of  $\gamma = 1$  and quantum number  $n = 3047$  is suspect, because if I have missed  $N$  levels, then  $2N$  spacings are wrong. This argues for taking a much smaller amount of levels, say 20, looking at this deviation, and being sure that no levels were

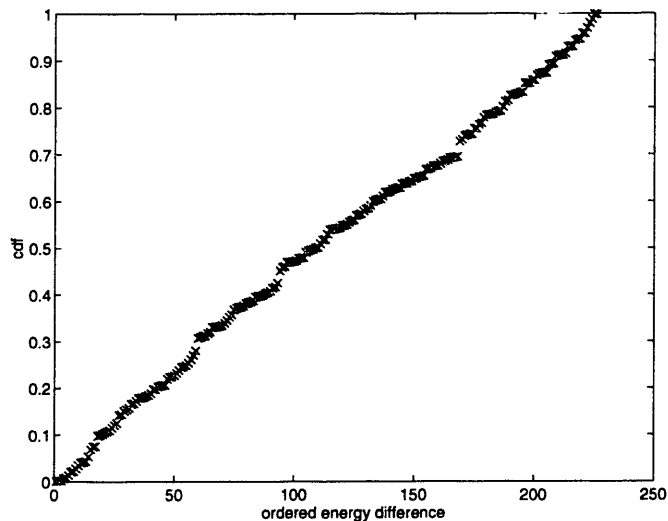


Figure 2-4: High energy band for aspect ratio one

missed. I wanted to verify a previous paper's results[20], so I have looked at another case of over a hundred levels. In all other cases, the amount of levels has been quite small and I have accepted the statistical uncertainty that a small number of levels entails. This approach is completely new to physicists. Normally, one needs on the order of three hundred levels to calculate statistics. I have found a way where you need less than fifty and can clearly show all deviations from the fit. I have shown that drawing histograms is not necessary to do, because it is possible to exactly compare the fit to the data.

Once I have the energy levels, I apply the iterative algorithm to obtain the necessary curve fit. Once I have the curve fit, I apply the E.D.F. statistics to find the confidence level of the fit. Now, my data should be linear for the fit, because the data should now be uniform. For the curve found, please see below 2-4 where I have plotted the c.d.f.  $F(y_i)$  vs.  $i$ .

Similarly one can see that the Brody distribution fits for a lower energy band 2-5 that substantially reproduces that found in an early paper on the stadium[20]. This reproduction gives weight to my results, because it reproduces a previous result.

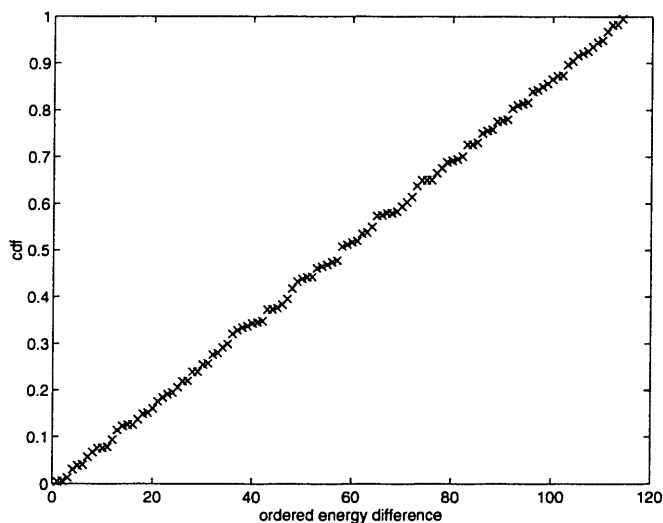


Figure 2-5: Low energy band for aspect ratio one

Moreover, the fit is clearly quite linear, so it is quite good.

Below, can be seen a smooth curve of the very low quantum number cases for the fit to the Brody distribution see fig. 2-6. In this case  $\gamma = 0.01$ . This rather strongly implies that the Brody distribution does not fit the curve at all; another distribution that fits the data. This curve also occurs in the other low quantum number case which strengthens the idea that another distribution describes the system.

For all the data calculated so far, please see the data below.

gamma	n	levels	w	significance
1	3047	241	0.88	0.9
1	405	112	0.95	0.95
0.1	380	32	0.71	0.9
0.1	30	16	0.91	0.75
0.01	30	16	0.73	0.75
0.001	340	16	0.43	0.9

The results of this table are plotted on the graph below 2-7. There are two interesting things to this plot. The first is that it is at  $\gamma = .1$  the state is already



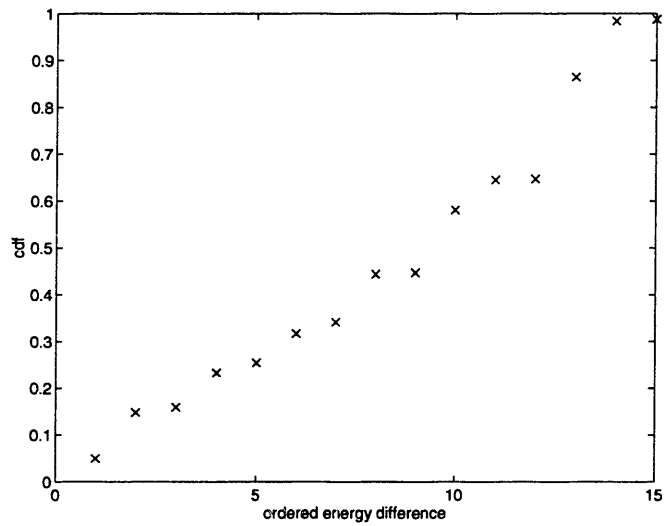


Figure 2-6: New distribution for low quantum numbers

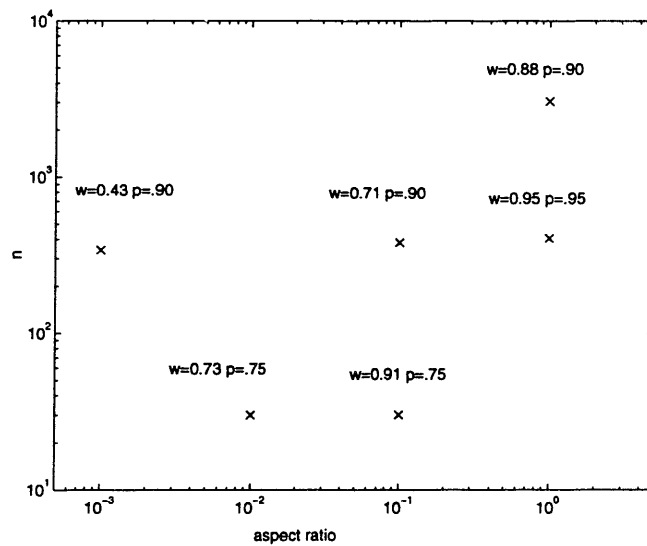


Figure 2-7: Goal of my thesis

mixed towards the Poisson distribution. This, of course, makes sense, because at  $\gamma = 0$ , the Brody distribution should have parameter 0. The second thing is the rather low confidence levels for the low quantum number cases which suggests another distribution may be the applicable one.

I have found a tentative functional relation between the Lyapunov exponent  $\lambda$  and the Brody parameter  $\omega$  of  $\lambda \log(\omega) \approx -0.05$ . This constant, I feel pretty confident, should be a function of the quantum number  $n$ , the energy eigenvalue number. This relationship does not hold for the low quantum number points, but, then, it does not seem appropriate if a different distribution is operating.

In conclusion, I have discovered a method that makes doing energy level statistics calculations quite a bit easier, because much less energy levels are needed. If there are many levels, a higher precision is obtained, because there is no lumping together of spacings. I have more than doubled the numerically investigated cases of the stadium. In so doing, I have been able to characterize to some extent the transition to chaos in the stadium billiard. I have found that for small quantum numbers, the energy level spacings do not seem to follow the Brody distribution. Lastly, I have found a tentative scaling law that relates the Brody parameter to the Lyapunov exponent, something that has never been done for any system before.

# Appendix A

## K-flows

I propose to give a lot of definitions to build up the machinery until I can define a K-flow. After each definition, I have endeavored to give an example. I have endeavored to structure this section by following the rule that the human mind likes to structure itself by considering about a half a dozen things at once[22]. I have borrowed heavily from two works for this section [26][2].

### A.1 $\sigma$ - algebra

A ring  $\mathcal{R}$  is a family of sets that has the following properties: if  $A$  and  $B \in \mathcal{R}$ , then

- i)  $A \cup B \in \mathcal{R}$
- ii)  $A - B \in \mathcal{R}$ .

An example of a ring is the collection of open sets inside a circle of radius one including the null set.

A  $\sigma$ -algebra is also a family of sets  $\mathcal{A}$  that has these properties:

- i) The null set is in  $\mathcal{A}$
- ii)  $\mathcal{A}$  is closed under complementation.
- iii)  $A_n \ n \in 1, 2, \dots \cup_{n=1}^{\infty} A_n \in \mathcal{A}$ .

The smallest  $\sigma$ -algebra that contains all open sets in  $R^d$  is the collection of all Borel sets. A set  $B$  is called a Borel set if it can be obtained by a countable number of unions, intersections, or complements of open sets. The previous example is not a

$\sigma$ -algebra. The union of open sets of radius  $\frac{n}{n+1}$  clearly is the entire circle including the boundary, but this is not inside the circle.

## A.2 measure space

Given a ring  $\mathcal{R}$ ,  $\phi$  is a set function defined on  $\mathcal{R}$  if  $(\forall A \in \mathcal{R}) \phi(A)$  is an extended real. The extended reals are the real numbers with  $\pm\infty$  added.  $\phi$  is non-negative if the number is always non-negative.  $\phi$  is additive if  $A \cap B = \emptyset \Rightarrow \phi(A \cup B) = \phi(A) + \phi(B)$ .  $\phi$  is countably additive if  $A_i \cap A_j = \emptyset (i \neq j) \Rightarrow \phi(\bigcup_{n=1}^{\infty} A_n) = \sum_{n=1}^{\infty} \phi(A_n)$ . Now, a non-negative countably additive set function is a measure. An example of a measure is the distance between points in  $R^d$ .

Given a set  $M$ , if a  $\sigma$ -ring of subsets  $\mathcal{M}$  of  $M$  exists and there is a measure  $\mu$  on  $\mathcal{M}$ ,  $M$  is called a measure space. An example of a measure space  $M$  could be the set of all positive integers.  $\mathcal{M}$  would be the collection of all subsets of  $M$ , commonly called the power set of  $M$ . For any  $A \in \mathcal{M}$   $\mu(A)$  is just the number of elements of  $A$ .

## A.3 abstract dynamical system

First, it is important to understand that with regard to abstract dynamical systems, it is not measure spaces that are important, but equivalence classes of measure spaces. For example, consider  $A$  and  $B \in \mathcal{B}$  and we define an equivalence relation.  $A = B(mod 0)$  if  $\mu(A \cup B - A \cap B) = 0$ . The equivalence class of the empty set includes all sets of measure zero. The quotient of  $\mathcal{B}$  under this equivalence relation is written as  $\mathcal{B}(mod 0)$ . Now given a measure space  $(M, \mu)$ ,  $\mu$  completely defines  $\mathcal{B}(mod 0)$ .

A homomorphism(mod 0) is a mapping  $\phi : M \rightarrow M'$  for two measure spaces  $(M, \mu)$  and  $(M', \mu')$  if it has the following properties:

- i) for  $\emptyset$ , a set a measure 0,  $\phi$  is defined on  $M - \emptyset$
- ii)  $\emptyset' = M' - \phi(M - \emptyset)$  has measure zero (A set that has measure zero is just what it sounds like  $\mu(\emptyset) = 0$ ). This means that  $\phi(M) = M'$  except for a measure zero subset of  $M'$

iii)  $\mu[\phi^{-1}(A)] = \mu'[A']$  for a representative of every equivalence class of  $\mathcal{B}$ . This means that  $\phi$  is measure preserving.

If both the mappings  $\phi$  and  $\phi^{-1}$  are homomorphisms(mod 0) and  $M$  is the same as  $M'$ , then  $\phi$  is called an automorphism(mod 0). An abstract dynamical system  $(M, \mu, \phi_t)$  is a measure space  $(M, \mu)$  with a group  $\phi_t$  of automorphisms(mod 0) on this space.  $\phi_t$  depends measurably on  $t$ .

## A.4 K-System

If we consider the algebra of all the measurable sets in a measure space. A subalgebra  $\mathcal{A}$  of measurable sets is a subset of this algebra which both contains  $M$  and is a  $\sigma$ -algebra itself.

An abstract dynamical system  $(M, \mu, \phi)$  is called a K-system if there exists a subalgebra  $\mathcal{A}$  that satisfies for any  $t \geq 0$ : i)  $\mathcal{A} \subset \phi\mathcal{A}$  ii) the algebra of sets of measure 0 or 1 is equal to the largest subalgebra which belongs to every  $\phi_t\mathcal{A}$  iii) the smallest subalgebra that contains every  $\phi_t\mathcal{A}$  is the complete algebra.

# Appendix B

## Modified version of Heller's program

---

```
PROGRAM STADIUM
IMPLICIT REAL*8 (A-H,O-Z)
DIMENSION A(190,180),W(180),V(180,180),B(190),X(180),XOLD(180)
  DIMENSION U(190,180),R(190),XX(190),YY(190)
  DIMENSION XK(180),YK(180),INIT(2)
CZI=(0.,1.)
PI = 3.1415926535897932384626433832795D0
```

10

```
c Ej Heller's plane wave basis for the stadium
c uses least squares singular value decomp.   Odd-odd only.
c see "numerical recipies" for more on the svd routines if
c stability or accuracy seems a problem.   (svd can be tuned
c with the w(i) criterion).
c There are N basis plane waves of wavevector mag.  TK
c and the wavfnc'n is set to zero at M places, M>N on the boundary
```

```
M=190
N=180
NP=180
MP=190
```

20

```

NPLOT=300
NP=180
XL=1.D0
TOL=1.D-4
TENEW = 0.
TENOL1=0.
TENOL2=0.
NP2=150

```

c XL is the length of the straight section

30

c TK is the wavevector magnitude

```

666   TK=1.
      NCOUNT=1
      OPEN(30, FILE= 'Half', STATUS = 'OLD')
      TKINC=0.
      NINC=2
      IMAN=0

```

c must balance wavevect. mag. with # basis fcns.

c TK too small is too unstable, too big permits leakage.

40

```

C   # BNDRY PTS, # BASIS FCNS, TK,XL, ISQ(2 GIVES PSI-SQUARED)'
      READ(30,*) M,N,TK,XL,ISQ
C   'TKINC, NINC, NPLOT,TOL'
      READ(30,*) TKINC,NINC,TOL

```

c apportion points between the straight sections

c and the quarter circle

```

      INIT(1)=((4+pi)/(1+pi))**(0.5)

```

c radius of the circle

50

```

      INIT(2)=.25*INIT(1)

```

c length of the straight section

```

      NTOP=NINT(INIT(2)*(M*INIT(2)/(1.57*INIT(1)+INIT(2))))+2
      NCIRC=M-NTOP

```

C COORDINATES OF THE POINTS TO BE SET TO ZERO

```

      DO I=1,NTOP

```

```

XX(I) = INIT(2)*(I-.5)/NTOP
YY(I) =INIT(1)
END DO

```

60

```

DO I=1,NCIRC
  XX(NTOP+I)= INIT(1)*DSIN((I-.5)*PI/NCIRC/2) + INIT(2)
  YY(NTOP+I)= INIT(1)*DCOS((I-.5)*PI/NCIRC/2)
END DO

```

544 CONTINUE

```

NCOUNT=NCOUNT+1
IF(NCOUNT.GT.NINC) then
GO TO 77
END IF
IF(TK.EQ.0.) GO TO 77

```

70

C THE BASIS SET WAVEVECTORS

```

TK=TK+TKINC
DO I=1,N
  XK(I) = TK* DCOS((I-.5)*PI/N/2)
  YK(I) = TK* DSIN((I-.5)*PI/N/2)
END DO

```

80

c set up the linear equations. ax=b. b is zero vector except for  
c last element. these equations are setting the wavefcn to zero on  
c the boundary, except the last one, (i=mp), which sets the wavefcn  
c to 0.1 at xs,ys

C

```

DO I=1,M-1
  DO J=1,N
    A(I,J) = DSIN(XK(J)*XX(I))*DSIN(YK(J)*YY(I))
    U(I,J)=A(I,J)
  END DO
END DO

```

90



```
XS=.325
YS=.43245
```

```
DO J=1,N
  A(M,J) = DSIN(XK(J)*XS)*DSIN(YK(J)*YS)
  U(M,J)=A(M,J)
END DO
```

100

c use singular value decomposition

```
CALL SVDCMP(U,M,N,MP,NP,W,V)
```

```
WMAX=0.
DO J=1,N
  IF(W(J).GT.WMAX)WMAX=W(J)
END DO
```

c !!!cutoff criterion here for W's!!!! 1.e-4 is conservative.

110

```
555          FORMAT(8E12.3)
          DET=1.
```

```
WMIN=WMAX*TOL
DO J=1,N
  IF(W(J).LT.WMIN) W(J)=0.
END DO
DO K=1,M
  B(K) = 0.DO
END DO
B(M)=.1
```

120

c these are the singular value matrix w's

c test the solution vector x on the original matrix:

```
CALL SVBKS(U,W,V,M,N,MP,NP,B,X)
```

```
DO I=1,M
  R(I)=0.
```

```

        DO K=1,N
            R(I)=R(I) + A(I,K)*X(K)
        END DO
    END DO

    RR=0.
    DO I=1,M-1
        RR=RR+R(I)**2
    END DO
    RR=RR+(R(M)-.1)**2
C   write(9,*) 'quality ',rr
c   check the value of the wavefcn where it was not
c   set to zero.
    TR=0.
    DO J=1,N
        TR=TR+X(J)*DSIN(XK(J)*XX(M))*DSIN(YK(J)*YY(M))
    END DO
c   check the sum squared of nctest+ntttest points on the
c   boundary. ideally, this should be zero but never will be.

    NTTEST=NTOP*4
    NCTEST=NCIRC*4
    TEST=0.
    DO I=1,NTTEST
        XTEST = INIT(2)*(I-.5)/NTTEST
        YTEST =INIT(1)
        TT=0.
        DO L=1,N
            TT=TT + X(L)*DSIN(XK(L)*XTEST)*DSIN(YK(L)*YTEST)
        END DO
        TEST = TEST+TT**2
    END DO

    DO I=1,NCTEST
        XTEST= INIT(1)*DSIN((I-.5)*PI/NCTEST/2) + INIT(2)
        YTEST= INIT(1)*DCOS((I-.5)*PI/NCTEST/2)
        TT=0.

```

```

      DO L=1,N
        TT=TT + X(L)*DSIN(XK(L)*XTEST)*DSIN(YK(L)*YTEST)
      END DO
    TEST = TEST+TT**2
  END DO
  WRITE(30,*) TK,TEST
c form matrix of wavefunction values
  GO TO 544

77  CONTINUE
  END

SUBROUTINE SVBKS(U,W,V,M,N,MP,NP,B,X)
  IMPLICIT REAL*8 (A-H,O-Z)

  PARAMETER (NMAX=190)
  DIMENSION U(MP,NP),W(NP),V(NP,NP),B(MP),X(NP),TMP(NMAX)
  DO 12 J=1,N
    S=0.
    IF(W(J).NE.0.)THEN
      DO 11 I=1,M
        S=S+U(I,J)*B(I)
11    CONTINUE
      S=S/W(J)
    ENDIF
    TMP(J)=S
12  CONTINUE
  DO 14 J=1,N
    S=0.
    DO 13 JJ=1,N
      S=S+V(J,JJ)*TMP(JJ)
13  CONTINUE
    X(J)=S
14  CONTINUE
  RETURN

```

**END**

**SUBROUTINE SVDCMP(A,M,N,MP,NP,W,V)**

**IMPLICIT REAL\*8 (A-H,O-Z)**

**PARAMETER (NMAX=190)**

**DIMENSION A(MP,NP),W(NP),V(NP,NP),RV1(NMAX)**

**G=0.0**

210

**SCALE=0.0**

**ANORM=0.0**

**DO 25 I=1,N**

**L=I+1**

**RV1(I)=SCALE\*G**

**G=0.0**

**S=0.0**

**SCALE=0.0**

**IF (I.LE.M) THEN**

**DO 11 K=I,M**

220

**SCALE=SCALE+DABS(A(K,I))**

11 **CONTINUE**

**IF (SCALE.NE.0.0) THEN**

**DO 12 K=I,M**

**A(K,I)=A(K,I)/SCALE**

**S=S+A(K,I)\*A(K,I)**

12 **CONTINUE**

**F=A(I,I)**

**G=-SIGN(DSQRT(S),F)**

**H=F\*G-S**

230

**A(I,I)=F-G**

**IF (I.NE.N) THEN**

**DO 15 J=L,N**

**S=0.0**

**DO 13 K=I,M**

**S=S+A(K,I)\*A(K,J)**

13 **CONTINUE**

```

        F=S/H
        DO 14 K=I,M
            A(K,J)=A(K,J)+F*A(K,I)
14          CONTINUE
15          CONTINUE
        ENDIF
        DO 16 K= I,M
            A(K )=SCALE*A(K,I)
16          CONTINUE
        ENDIF
    ENDIF
    W(I)=SCALE *G
    G=0.0
    S=0.0
    SCALE=0.0
    IF ((I.LE.M).AND.(I.NE.N)) THEN
        DO 17 K=L,N
            SCALE=SCALE+DABS(A(I,K))
17          CONTINUE
        IF (SCALE.NE.0.0) THEN
            DO 18 K=L,N
                A(I,K)=A(I,K)/SCALE
                S=S+A(I,K)*A(I,K)
18            CONTINUE
            F=A(I,L)
            G=-SIGN(DSQRT(S),F)
            H=F*G-S
            A(I,L)=F-G
            DO 19 K=L,N
                RV1(K)=A(I,K)/H
19            CONTINUE
            IF (I.NE.M) THEN
                DO 23 J=L,M
                    S=0.0
                    DO 21 K=L,N
                        S=S+A(J,K)*A(I,K)

```

```

21     CONTINUE
      DO 22 K=L,N
        A(J,K)=A(J,K)+S*RV1(K)
22     CONTINUE
23     CONTINUE
      ENDIF
      DO 24 K=L,N
        A(I,K)=SCALE*A(I,K)
24     CONTINUE
      ENDIF
      ENDIF
      ANORM=MAX(ANORM,(DABS(W(I))+DABS(RV1(I))))
25     CONTINUE
      DO 32 I=N,1,-1
        IF (I.LT.N) THEN
          IF (G.NE.0.0) THEN
            DO 26 J=L,N
              V(J,I)=(A(I,J)/A(I,L))/G
26     CONTINUE
            DO 29 J=L,N
              S=0.0
              DO 27 K=L,N
                S=S+A(I,K)*V(K,J)
27     CONTINUE
              DO 28 K=L,N
                V(K,J)=V(K,J)+S*V(K,I)
28     CONTINUE
29     CONTINUE
            ENDIF
            DO 31 J=L,N
              V(I,J)=0.0
              V(J,I)=0.0
31     CONTINUE
            ENDIF
            V(I,I)=1.0
            G=RV1(I)

```

```

L=I
32 CONTINUE
DO 39 I=N,1,-1
L=I+1
G=W(I)
IF (I.LT.N) THEN
DO 33 J=L,N
A(I,J)=0.0
33 CONTINUE
ENDIF
IF (G.NE.0.0) THEN
G=1.0/G
IF (I.NE.N) THEN
DO 36 J=L,N
S=0.0
DO 34 K=L,M
S=S+A(K,I)*A(K,J)
34 CONTINUE
F=(S/A(I,I))*G
DO 35 K=I,M
A(K,J)=A(K,J)+F*A(K,I)
35 CONTINUE
36 CONTINUE
ENDIF
DO 37 J=I,M
A(J,I)=A(J,I)*G
37 CONTINUE
ELSE
DO 38 J= I,M
A(J,I)=0.0
38 CONTINUE
ENDIF
A(I,I)=A(I,I)+1.0
39 CONTINUE
DO 49 K=N,1,-1
DO 48 ITS=1,30

```

```

DO 41 L=K,1,-1
  NM=L-1
  IF ((DABS(RV1(L))+ANORM).EQ.ANORM) GO TO 2
  IF ((DABS(W(NM))+ANORM).EQ.ANORM) GO TO 1
41  CONTINUE
1   C=0.0
    S=1.0
    DO 43 I=L,K
      F=S*RV1(I)
      IF ((DABS(F)+ANORM).NE.ANORM) THEN
        G=W(I)
        H=DSQRT(F*F+G*G)
        W(I)=H
        H=1.0/H
        C= (G*H)
        S=-(F*H)
        DO 42 J=1,M
          Y=A(J,NM)
          Z=A(J,I)
          A(J,NM)=(Y*C)+(Z*S)
          A(J,I)=-(Y*S)+(Z*C)
42  CONTINUE
      ENDIF
43  CONTINUE
2   Z=W(K)
    IF (L.EQ.K) THEN
      IF (Z.LT.0.0) THEN
        W(K)=-Z
        DO 44 J=1,N
          V(J,K)=-V(J,K)
44  CONTINUE
      ENDIF
      GO TO 3
    ENDIF
    IF (ITS.EQ.30) PAUSE 'No convergence in 30 iterations'
    X=W(L)

```



```

NM=K-1
Y=W(NM)
G=RV1(NM)
H=RV1(K)
F=((Y-Z)*(Y+Z)+(G-H)*(G+H))/(2.0*H*Y)
G=DSQRT(F*F+1.0)
F=((X-Z)*(X+Z)+H*((Y/(F+SIGN(G,F)))-H))/X
C=1.0
S=1.0
DO 47 J=L,NM
    I=J+1
    G=RV1(I)
    Y=W(I)
    H=S*G
    G=C*G
    Z=DSQRT(F*F+H*H)
    RV1(J)=Z
    C=F/Z
    S=H/Z
    F= (X*C)+(G*S)
    G=-(X*S)+(G*C)
    H=Y*S
    Y=Y*C
DO 45 NM=1,N
    X=V(NM,J)
    Z=V(NM,I)
    V(NM,J)= (X*C)+(Z*S)
    V(NM,I)=- (X*S)+(Z*C)
45    CONTINUE
Z=DSQRT(F*F+H*H)
W(J)=Z
IF (Z.NE.0.0) THEN
    Z=1.0/Z
    C=F*Z
    S=H*Z
ENDIF

```

390

400

410

```

      F= (C*G)+(S*Y)
      X=-(S*G)+(C*Y)
      DO 46 NM=1,M
      Y=A(NM,J)
      Z=A(NM,I)
      A(NM,J)= (Y*C)+(Z*S)
      A(NM,I)=- (Y*S)+(Z*C)
46    CONTINUE
47    CONTINUE
      RV1(L)=0.0
      RV1(K)=F
      W(K)=X
48    CONTINUE
3     CONTINUE
49    CONTINUE
      RETURN
      END

```

DOUBLE PRECISION FUNCTION RAN1(IDUM)

IMPLICIT REAL\*8 (A-H,O-Z)

DIMENSION R(97)

PARAMETER (M1=259200,IA1=7141,IC1=54773,RM1=3.8580247E-6)

PARAMETER (M2=134456,IA2=8121,IC2=28411,RM2=7.4373773E-6)

PARAMETER (M3=243000,IA3=4561,IC3=51349)

DATA IFF /0/

IF (IDUM.LT.0.OR.IFF.EQ.0) THEN

IFF=1

IX1=MOD(IC1-IDUM,M1)

IX1=MOD(IA1\*IX1+IC1,M1)

IX2=MOD(IX1,M2)

IX1=MOD(IA1\*IX1+IC1,M1)

IX3=MOD(IX1,M3)

DO 11 J=1,97

IX1=MOD(IA1\*IX1+IC1,M1)

IX2=MOD(IA2\*IX2+IC2,M2)

```
      R(J)=(FLOAT(IX1)+FLOAT(IX2)*RM2)*RM1
11  CONTINUE
      IDUM=1
      ENDIF
      IX1=MOD(IA1*IX1+IC1,M1)
      IX2=MOD(IA2*IX2+IC2,M2)
      IX3=MOD(IA3*IX3+IC3,M3)
      J=1+(97*IX3)/M3
      IF(J.GT.97.OR.J.LT.1)PAUSE
      RAN1=R(J)
      R(J)=(FLOAT(IX1)+FLOAT(IX2)*RM2)*RM1
      RETURN
      END
```

460

# Bibliography

- [1] D. Alonso and P. Gaspard. Role of the edge orbits in the semiclassical quantization of the stadium billiard. *J. Phys. A*, 27:1599–1607, 1994.
- [2] V.I. Arnold and A. Avez. *Ergodic Problems of Classical Mechanics*. Addison-Wesley, New York, 1989.
- [3] N. Balazs and A. Voros. Chaos on the pseudosphere. *Physics Reports*, 143:109+.
- [4] R. Balescu. *Equilibrium and Non-Equilibrium Statistic Mechanics*. John Wiley and Sons, New York, 1975.
- [5] G. Benettin and J.-M. Strelcyn. Numerical experiments of a point mass moving in a plane convex region: Stochastic transition and entropy. *Phy. Rev. A*, 17:773–785, 1978.
- [6] M. Berry. *J. Phys. A*, 10:2083+, 1977.
- [7] O. Bohigas. Random matrix theories and chaotic dynamics. In M.-J. Giannoni, A. Voros, and J. Zinn-Justin, editors, *Chaos et Physique Quantique*, number 52 in Les Houches, part 2, pages 100–102. Elsevier Science Publishers, New York, 1991.
- [8] O. Bohigas, M.J. Giannoni, and C. Schmidt. Characterization of chaotic quantum spectra and universality of level fluctuation laws. *Phys. Rev. Lett.*, 52:1–3, 1984.
- [9] O. Bohigas, M.J. Giannoni, and C. Schmidt. Spectral properties of the laplacian and random matrix theories. *J. Physique Lett.*, 45:L-1015 – L-1022, 1984.

- [10] O. Bohigas and Giannoni M.-J. Chaotic motion and random matrix theories. In M. Dietrich, M. Di Toro, and H.J. Mang, editors, *Proceedings of the Winter College on Fundamental Nuclear Physics*, number 3, pages 1871–1972. World Scientific, Singapore.
- [11] T. Brody, J. Flores, J. French, P Mello, A. Pandey, and S. Wong. Random-matrix physics: spectrum and strength fluctuations. *Rev. Mod. Phys.*, 53:385+, 1981.
- [12] L.A. Bunimovich. On ergodic properties of certain billiards. *Funct. Anal. App.*, 8:254+, 1974.
- [13] L.A. Bunimovich. On the ergodic properties of nowhere dispersing billiards. *Commun. Math Phys.*, 65:295–312, 1979.
- [14] K.M. Christoffel and P. Brumer. Quantum and classical dynamics in the stadium billiard. *Phys. Rev. A*, 33:1309–1321, 1986.
- [15] H. Graf and et al. Distribution of eigenmodes in a superconducting stadium billiard with chaotic dynamincs. *Phy. Rev. Lett.*, 69:1296–1299, 1992.
- [16] M. Gutzwiller. *Chaos in Classical and Quantum Mechanics*. Springer-Verlag, New York, 1990.
- [17] E. Heller. Wavepacket dynamics and quantum chaology. In M.-J. Giannoni, A. Voros, and J. Zinn-Justin, editors, *Chaos et Physique Quantique*, number 52 in Les Houches, part 9, pages 548–663. Elsevier Science Publishers, New York, 1991.
- [18] R. Horn and C. Johnson. *Topics in Matrix Analysis*. Cambridge University Press, New York, 1991.
- [19] C. Kruelle, A. Kittel, and R. Huebener. Nonintegrable stadium billiard seen as a mirror cabinet. *Z. Naturforsch*, 48:1039–1040, 1993.

- [20] S.W. McDonald and A.N. Kaufman. Spectrum and eigenfunctions for a hamiltonian with stochastic trajectories. *Phys. Rev. Lett.*, 18:1189–1191, 1979.
- [21] S.W. McDonald and A.N. Kaufman. Wave chaos in the stadium: Statistical properties of short-wave solutions of the helmholtz equation. *Phys. Rev. A*, 37:3067–3086, 1988.
- [22] G. Miller. The magical number seven plus or minus two. *Psychological Review*, 63:81+, 1956.
- [23] D. Moore. Tests of chi-squared type. In R. D’Agostino and M. Stephens, editors, *Goodness-of-Fit Techniques*, number 68 in *Statistics: textbooks and monographs*, part 3, pages 69–70. Marcel Dekker, New York, 1986.
- [24] G. Parisi. *Statistical Field Theory*. Addison-Wesley, Reading, Mass., 1988.
- [25] W. Press, S. Teukolsky, W. Vetterling, and B. Flannery. *Numerical Recipes in C*. Cambridge University Press, New York, 1992.
- [26] W. Rudin. *Principles of Mathematical Analysis*. McGraw-Hill, New York, 1976.
- [27] M. Sieber, U. Smilansky, S.C. Creagh, and R.G. Littlejohn. Non-generic spectral statistics in the quantized stadium billiard. *J. Phys. A*, 26:6217–6230, 1993.
- [28] M. Stephens. Tests based on e.d.f. statistics. In R. D’Agostino and M. Stephens, editors, *Goodness-of-Fit Techniques*, number 68 in *Statistics: textbooks and monographs*, chapter 4. Marcel Dekker, New York, 1986.
- [29] R. Taylor and P. Brumer. *Faraday Discuss. Chem. Soc.*, 75:115+, 1983.
- [30] S. Tomosovic and E. Heller. Long-time semiclassical dynamics of chaos: The stadium billiard. *Phys. Rev. E*, 47:282–299, 1993.

# THESIS PROCESSING SLIP

FIXED FIELD: ill. \_\_\_\_\_ name \_\_\_\_\_

index \_\_\_\_\_ biblio \_\_\_\_\_

► COPIES: Archives Aero Dewey Eng Hum  
Lindgren Music Rotch Science

TITLE VARIES: ►  \_\_\_\_\_

NAME VARIES: ►  \_\_\_\_\_

IMPRINT: (COPYRIGHT) \_\_\_\_\_

► COLLATION: 46 p

► ADD. DEGREE: \_\_\_\_\_ ► DEPT.: \_\_\_\_\_

SUPERVISORS: \_\_\_\_\_

NOTES:

cat'r:

date:

► DEPT: Phy

page:
► J174

► YEAR: 1995 ► DEGREE: M.S.

► NAME: GLOSS, David Samuel